Effect of active neurons in coupled neuronal networks

Ankita

MS15146

*A dissertation submitted for the partial fulfilment
of BS-MS dual degree in Science*

Indian Institute of Science Education and Research Mohali
April 2020

Certificate of Examination

This is to certify that the dissertation titled **"Effect of active neurons in coupled neuronal networks"** submitted by **Ankita** (Reg. No. MS15146) for the partial fulfillment of BS-MS dual degree programme of the Institute, has been examined by the thesis committee duly appointed by the Institute. The committee finds the work done by the candidate satisfactory and recommends that the report be accepted.

Prof.Rajeev Kapri   Prof. Sanjeev Kumar   Prof. Abhishek Chaudhari
(Supervisor)

Dated: May 4, 2020

Declaration

The work presented in this dissertation has been carried out by me under the guidance of Prof. Sudeshna Sinha and Prof. Abhishek Chaudhuri at the Indian Institute of Science Education and Research Mohali and Prof. Punit Parmananda at the Indian Institute of Technology Bombay.
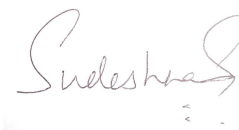
This work has not been submitted in part or in full for a degree, a diploma, or a fellowship to any other university or institute. Whenever contributions of others are involved, every effort is made to indicate this clearly, with due acknowledgment of collaborative research and discussions. This thesis is a bonafide record of original work done by me and all sources listed within have been detailed in the bibliography.

Ankita

Ankita

(Candidate)

Dated: May 4, 2020

In my capacity as the supervisor of the candidate's project work, I certify that the above statements by the candidate are true to the best of my knowledge.
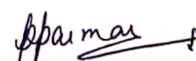
Prof. Sudeshna Sinha

Indian Institute of Science Education and Research Mohali

(Thesis Supervisor)

In my capacity as the supervisor of the candidate's project work, I certify that the above statements by the candidate are true to the best of my knowledge.

Prof. Abhishek Chaudhuri

Indian Institute of Science Education and Research Mohali

(Internal Supervisor)

In my capacity as the supervisor of the candidate's project work, I certify that the above statements by the candidate are true to the best of my knowledge.

Prof. Punit Parmananda

Indian Institute of Technology Bombay

(External Supervisor)

Acknowledgment

List of Figures

Abstract

The neurons have earlier been modeled using various dynamic equations and the emergence of collective behaviors has been investigated in coupled neuronal systems. In this thesis, we try to model neurons as the discrete dynamical system, using maps or the continuous-time dynamical system, using differential equations. These model neurons could be intrinsically active or inactive. Therefore, the model governing the dynamics of these neurons should display a rich dynamical behavior so that we could characterize the active and inactive state of the neuron. These model neurons are then coupled to each other using different coupling forms. First, we try to see the fraction of neurons exhibiting activity in the emergent dynamics as a function of coupling strength and the fraction of intrinsically active neurons in a neuronal network or population. Then we try to see the emergent patterns in the two coupled neuronal sub-populations. We investigate the effect of connection density, inter-group coupling and population size on the collective dynamical patterns.

Contents

Chapter 1

Introduction

As the word describes itself, the systems which evolve with time are called dynamical systems. It can be represented using differential equations or difference equations. These equations which describe nonlinear dynamical systems have some additional nonlinear terms which make their analysis difficult. The nonlinear systems may be hard to accurately model, even if they are deterministic. Nonlinear systems (continuous) of order equal to or greater than three show interesting dynamics which we call chaos. A dynamical system is chaotic if its future behavior is highly sensitive to initial conditions. In such dynamical systems, two very close initial conditions would give rise to different and uncorrelated dynamics. It makes the prediction of the evolution of the system impossible and gives rise to unpredictability. The butterfly effect is the phenomenon that describes the unpredictability of deterministic dynamical systems that is how a small change in the initial condition may give rise to a large deviation in the later stages of the system.

The equations governing dynamical systems may be continuous or discrete. A continuous-time system is described by differential equations. For instance, a dynamical system of dimension N given by *ordinary differential equations* has the following form:

$$\frac{d\mathbf{x}}{dt} = \mathbf{f}(\mathbf{x})$$

where $\mathbf{x}$ is a N-dimensional vector denoting the N state variables of the system, and $\mathbf{f} \equiv \{f_1, f_2 \dots f_N\}$ are functions describing the time evolution of these variables. The fixed point of the dynamics, also known as the steady state or equilibrium, is the time-invariant state where there is no further change in the variables in time. So the fixed point in a continuous-time system corresponds to $\frac{d\mathbf{x}}{dt} = 0$

On the other hand, *maps* describe a class of dynamical systems in which time is discrete rather than continuous. They are described using difference equations and are mathematical operators that advance the system by a one-time step.

$$\mathbf{x}_{n+1} = \mathbf{f}(\mathbf{x}_n)$$

Here $\mathbf{x}_n$ is a vector denoting the state variables of the system at time step n and $\mathbf{f}$ is the map giving the relation between the state at time n and the state at the next time step $n + 1$. The sequence $\mathbf{x}_0, \mathbf{x}_1, \mathbf{x}_2 \dots$, also called iterates, is the orbit starting from $\mathbf{x}_0$ which is the initial state at time $n = 0$. If $\mathbf{x}^* = \mathbf{f}(\mathbf{x}^*)$, then $\mathbf{x}^*$ is a fixed point that is, if $\mathbf{x}_n = \mathbf{x}^*$ then $\mathbf{x}_{n+1} = \mathbf{f}(\mathbf{x}_n) = \mathbf{f}(\mathbf{x}^*) = \mathbf{x}^*$, therefore the orbit remains at $\mathbf{x}^*$ for all the future iterations[Str01].

Now we describe below the different dynamical systems we have explored in this thesis.

1.1 Chialvo Map

Chialvo map is a two-dimensional map describing the evolution of a two-dimensional system (i.e. a system whose state $\mathbf{x}$ has two components, $\{x, y\}$). It is capable of displaying rich dynamics, and is given by the following dynamical equations [Chi95]:

$$
\begin{aligned}
x_{n+1} &= f_1(x_n, y_n) = x_n^2 exp(y_n - x_n) + k \\
y_{n+1} &= f_2(x_n, y_n) = ay_n - bx_n + c
\end{aligned}
\tag{1.1}
$$

Here, x_n denotes the activation variable, and y_n denotes the recovery variable in the context of the biological systems.

Parameters k and c are offsets to the variables x_n and y_n while a is the rate constant for y_n and b is the activation dependence of the recovery variable as it relates y_n to x_n.

As the parameters of the map are varied, the qualitative structure of the flow changes. In particular, fixed points can be created or destroyed, or their stability may change. The qualitative changes in the dynamics are called bifurcations. For example, if a parameter is varied, at one value, it may give a fixed point attractor, while at another value, it may change it to a periodic orbit attractor and such a critical parameter is called bifurcation parameter.[Str01]

Here, the attractor is defined as a set of numerical values toward which a system tends to evolve, for a wide variety of starting conditions of the system.

The bifurcation diagram for the Chialvo map with respect to the bifurcation parameter, k, is as shown in figure 1.1. The parameters used are: $a = 0.89, b = 0.18, c = 0.28$.
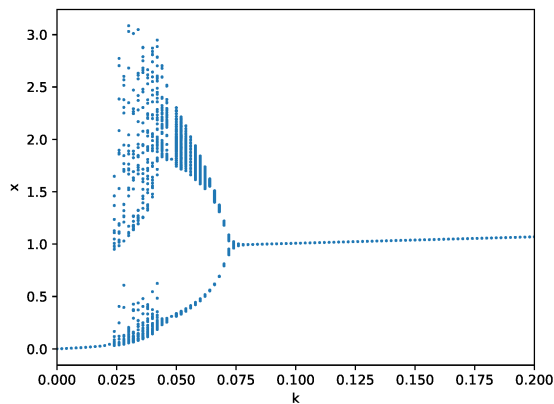
Figure 1.1: Bifurcation diagram for Chialvo map with respect to k

For a range of bifurcation parameter, k, it displays fixed point to chaotic to periodic behavior for different values of k. This bifurcation has been plotted using Poincaré section. For a Poincaré section, an arbitrary plane is taken which cuts the attractor into two pieces. Therefore, the orbits comprising

the attractor crosses the plane several times and the intersections of the orbits and Poincare plane is plotted. Poincaré section hence reveals the structure of the attractor.

This two-dimensional map has been widely used to model the dynamics of isolated neurons and in Coupled Map Lattices to represent neural networks.

The active and inactive state of a neuron is established using the parameters of the Chialvo map. If the time series of a model neuron is either spiking or bursting, it is defined as an active neuron. The parameters used for spiking are: $a = 0.89, b = 0.6, c = 0.28, k = 0.03$.
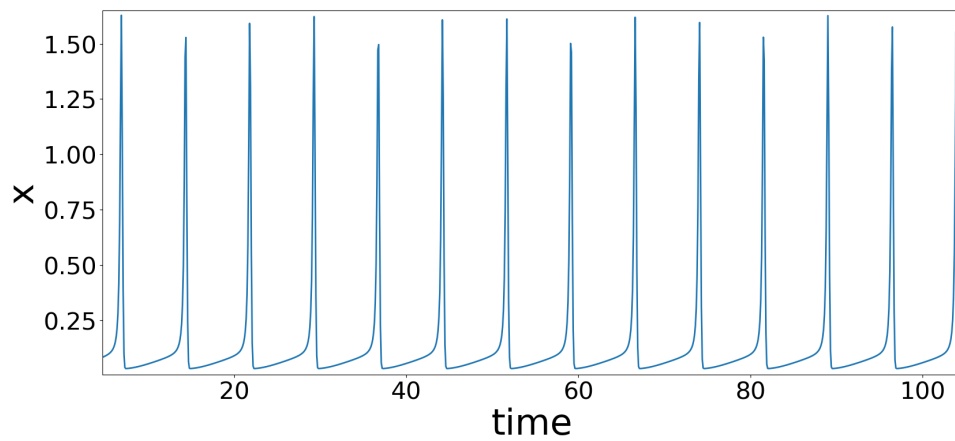
Figure 1.2: Spiking of a neuron(active state)

The parameters used for bursting are: $a = 0.89, b = 0.18, c = 0.28, k = 0.04$.
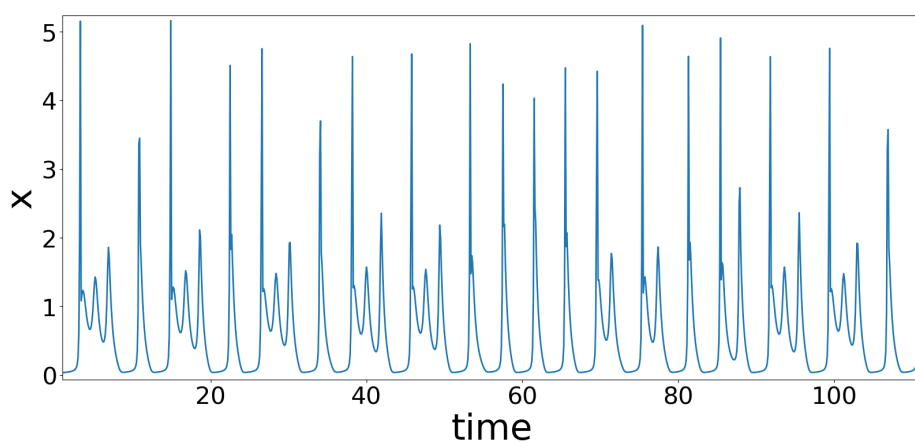
Figure 1.3: Bursting of a neuron(Active state)

3

While, if the time series of a model neuron is a fixed point, it is defined as an inactive neuron. The parameters used for a system exhibiting a fixed point are: $a = 0.89, b = 0.18, c = 0.28, k = 0.1$.
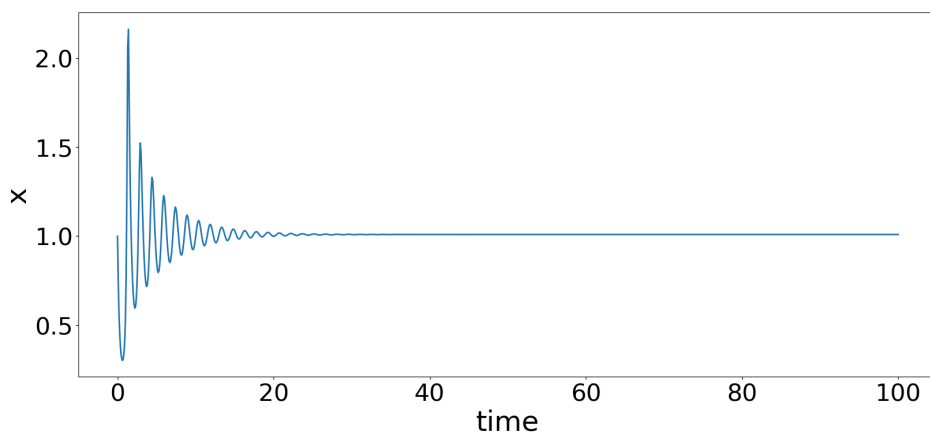
Figure 1.4: Inactive state of a neuron

In our analysis, the bifurcation parameter, k, is kept in either chaotic or periodic region for an active neuron, while for an inactive neuron it is kept in the fixed point region.

1.2 Different forms of coupling

Coupled systems are often found in nature, which interact with each other to display collective behavior. Different types of interaction or coupling forms used in this thesis are :

Table 1.1: Coupling forms

Type of Coupling	Functional form
Diffusive Repulsive	$(x_j + x_i)$
Diffusive Attractive	$(x_j - x_i)$
Mean field	$(\overline{x_j} - x_i)$

1.3 Mercury Beating Heart System

The mercury beating heart is a chemo-mechanical oscillator that can be used to envision various phenomena exhibited by different oscillators existing in nature. It is the result of the electrochemical redox reaction between Mercury and Iron kept in an electrolyte solution. The setup of the MBH system as shown in figure 1.5, consists of a mercury drop in the aqueous solution of an acid and strong oxidant in a concave watch glass. A pointed iron nail is made to touch the periphery of the mercury drop, which then triggers the mechanical oscillations in the system. The mechanical oscillations in

the MBH system look similar to that of a beating heart, that's why it is known as mercury beating heart system. It is a chemo-mechanical oscillator because the interplay between the chemical and mechanical oscillations causes the self-sustained oscillations in the system. In particular, the chemical redox reactions on the surface of the mercury and the change in surface tension of the mercury drop drive the system to oscillate mechanically [Avn89].
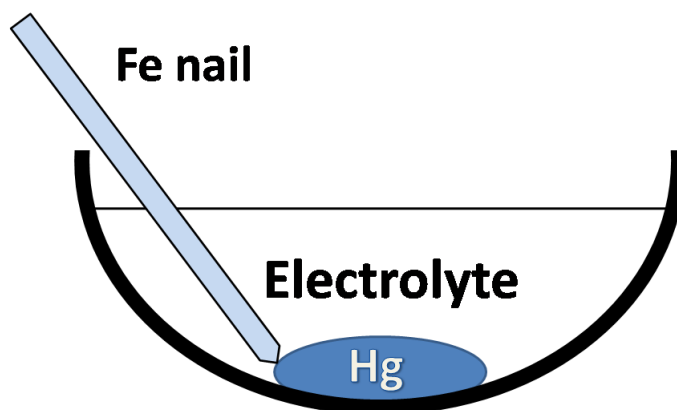
Figure 1.5: Mercury Beating Heart setup

1.4   Basic Mechanism of Oscillation in the MBH system

Mercury is a metal that exists as a liquid and has very high density and surface tension at room temperature. The oscillations in the MBH system originate from the oxidation of mercury surface by the oxidizing agent, cerium sulfate, followed by the reduction of the oxide back to mercury by iron. These processes affect the surface tension and ultimately the geometry of the mercury drop.

In a watch glass, 2 ml of mercury(Hg), 6M of sulphuric acid(H_2SO_4), and 6M of cerium sulfate were placed.

In the presence of 6M sulphuric acid, cerium exists as $[Ce^{IV}(SO_4)_3]^{2-}$ which acts as the oxidizing agent.[CRBV02]

$$Ce(SO_4)_2 + SO_4(aq) \rightleftharpoons [Ce^{IV}(SO_4)_3]^{2-}$$
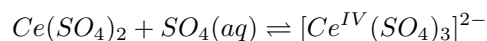
$[Ce^{IV}(SO_4)_3]^{2-}$ then reacts with metallic Hg, according to the following reactions:

$$2[Ce^{IV}(SO_4)_3]^{2-} + 2Hg \rightleftharpoons Hg_2^{2+} + 2[Ce^{III}SO_4]^+ + 4SO_4^{2-}(aq)$$

$$2[Ce^{IV}(SO_4)_3]^{2-} + 2Hg \rightleftharpoons Hg_2SO_4 + 2[Ce^{III}SO_4]^+ + 3SO_4^{2-}(aq)$$
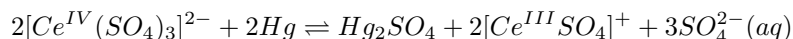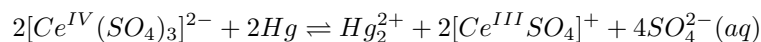
Here Hg_2^{2+} is the free ion, Hg_2SO_4 is the molecular mercury(I) sulfate. The metallic Fe can undergo the following reactions

$$Fe + Hg_2^{2+} \rightleftharpoons Fe^{2+}(aq) + 2Hg$$

5

$$Fe + Hg_2SO_4 \rightleftharpoons Fe^{2+}(aq) + 2Hg + SO_4^{2-}(aq)$$
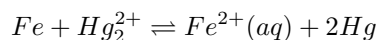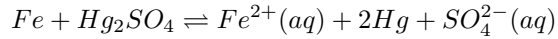
In the presence of the oxidizing agent, mercury oxidizes accumulating the positive charge on its surface. The repulsion of like charges causes a reduction in the surface tension which leads to the expansion of the mercury surface. Once, the iron nail is touched to the surface of mercury, the mercury is reduced while leaving the iron oxidized. The mercury surface gets discharged raising the surface tension which then leads to the compression of the mercury surface.

Therefore, a series of redox reactions and surface tension interplay to cause the beating heart motion of the mercury.

1.5 FitzHugh-Nagumo model

FitzHugh-Nagumo model is a mathematical model of neuronal excitability developed by Richard FitzHugh [Fit61]. It is a simplified version of the Hodgkin-Huxley model which models the activation and deactivation dynamics of a spiking neuron. It consists of two coupled, nonlinear differential equations. It is a continuous-time dynamical system, unlike the Chialvo map.

The equations describing the dynamics of the system is given by:

$$\begin{aligned}
\frac{dv_i}{dt} &= v_i - \frac{v_i^3}{3} - \omega_i + I_{ext} \\
\tau\frac{d\omega_i}{dt} &= v_i + a - b\omega_i
\end{aligned}$$
(1.2)

Here, v is the membrane voltage and ω is the recovery variable, I_{ext} is the external stimulus, and a and b and τ are dimensionless, positive, and used for the time scale and kinetics of the recovery variable.

The first equation describes the fast evolution of the neuronal membrane voltage and the other one describes the slower recovery action of the sodium and potassium channel

The bifurcation diagram for the FHN model with respect to the bifurcation parameter, current (I_{ext}) is given by:
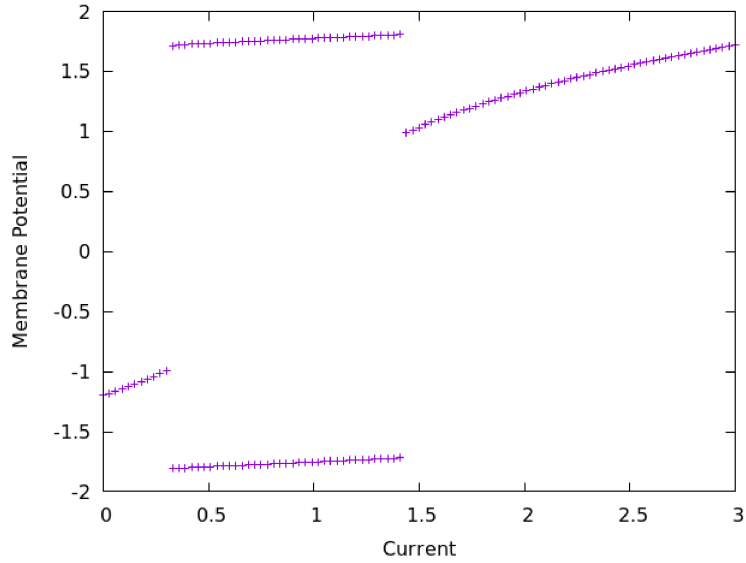
Figure 1.6: Bifurcation diagram for FHN model with respect to I_{ext}

It displays fixed point and period-1 cycle behavior in the different ranges of current. The region of the current where there are two lines denotes the period-1 cycle region whereas the single line in the space denotes the fixed point region. For an active neuron, we keep the current in period-1 region while for an inactive neuron we keep the current in fixed point region.

The active and inactive state of the neuron is established by keeping $a = 0.7, b = 0.8$ and $\frac{1}{\tau} = 0.08$ constant while changing the value of current (I_{ext}) according to the bifurcation diagram.

If the time series of the model neuron is periodic, it is defined as an active neuron. The parameters used are: $a = 0.7, b = 0.8, \frac{1}{\tau} = 0.08$ and $I_{ext} = 1.0$
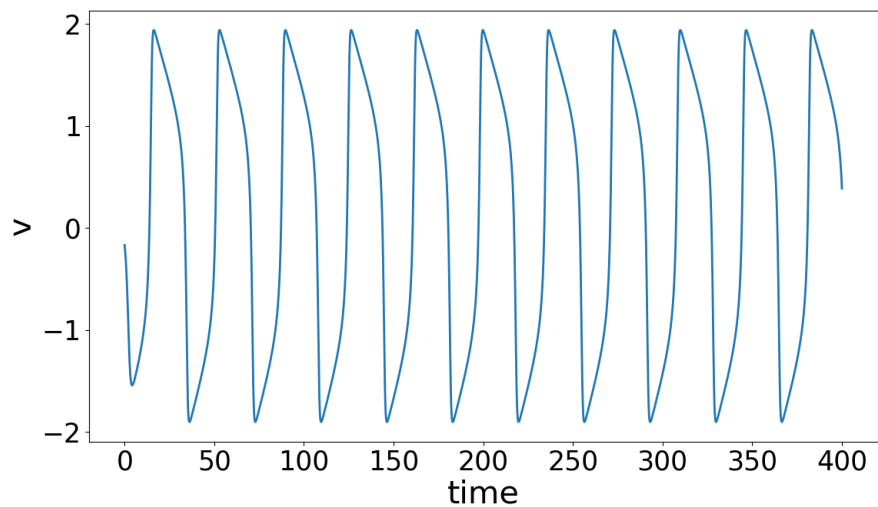
Figure 1.7: Time series of an active oscillator

If $\frac{1}{\tau}$ is changed while keeping the other parameters constant, just the frequency of oscillation changes. For example, if $\frac{1}{\tau} = 0.3$, the time series looks like, Figure 1.8.
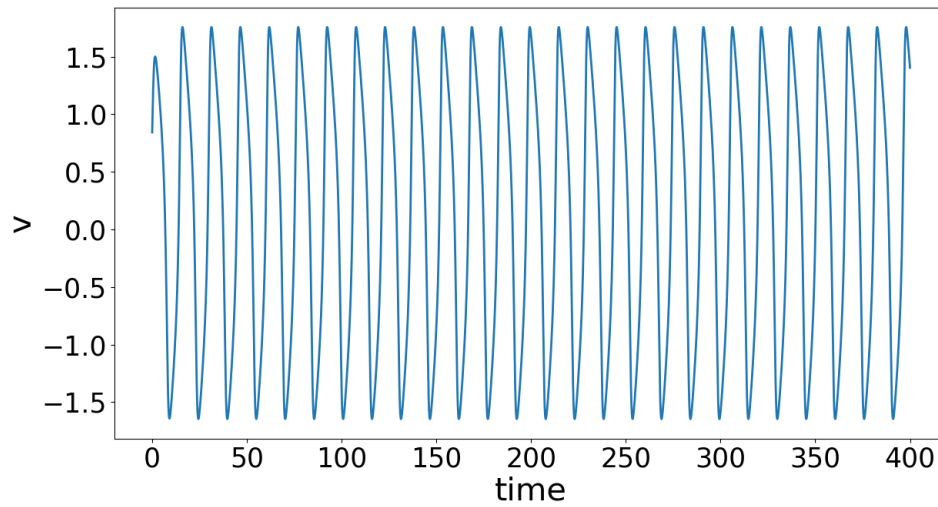
Figure 1.8: Time series of an active oscillator

Also, the time series of an inactive neuron looks like Fig 1.9. The parameters used are: $a = 0.7, b = 0.8, \frac{1}{\tau} = 0.08$ and $I_{ext} = 0.1$
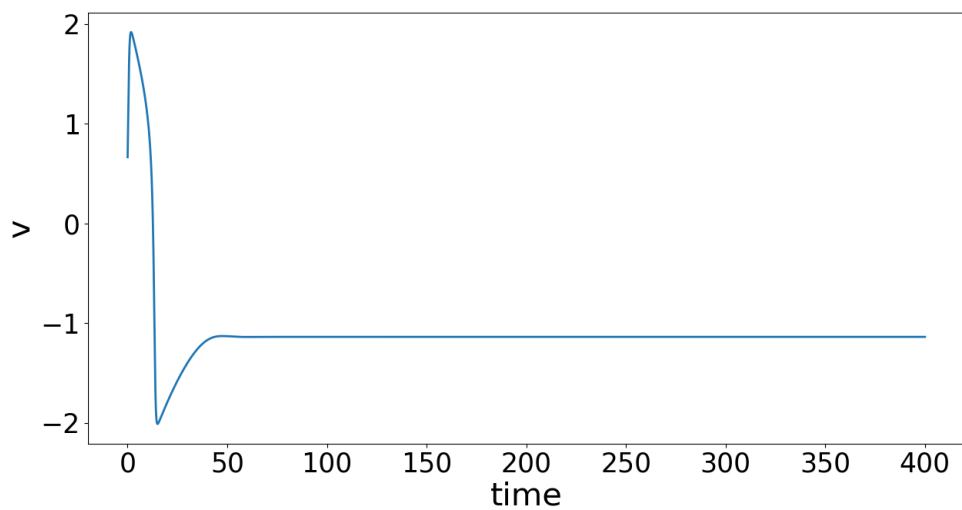
Figure 1.9: Time series of an inactive oscillator

Chapter 2

Nearest neighbor coupled neuronal network

Coupled Map Lattices (CML) have been used as effective models for spatiotemporal phenomena in complex systems ranging from biology to engineering for almost two decades[Kan93]. In general, CMLs consist of collections of on-site maps reflecting local nonlinearities, interacting with neighboring sites through different types of coupling forms. Here, the CML approach is used to model a ring of neurons using the two-dimensional nonlinear Chialvo map, capable of displaying dynamical behavior ranging in complexity from fixed points (inactive state) to chaos (active state), as a local dynamical unit.

These model neurons which may be intrinsically active or inactive are coupled to their nearest neighbors. The effect of active neurons (f) on the collective dynamical patterns is studied as a function of the fraction of intrinsically active neurons and the coupling strength.

2.1 Model

We consider a one – dimensional ring of neurons modeled by the two-dimensional map known as Chialvo Map[Chi95]. This map will determine the local dynamics of our system. It is defined as:

$$
\begin{aligned}
x_{n+1} &= f_1(x_n, y_n) = x_n^2 exp(y_n - x_n) + k \\
y_{n+1} &= f_2(x_n, y_n) = ay_n - bx_n + c
\end{aligned}
\tag{2.1}
$$

x_n denotes the activation variable and y_n denotes recovery variable in the context of the biological systems.

Parameters k and c are offsets to the variables x_n and y_n while a is the rate constant for y_n and b is the activation dependence of the recovery variable as it relates y_n to x_n.

For active state of neurons we have used the parameters:

$$a = 0.89, b = 0.18, c = 0.28, k = 0.04$$

For inactive state of neurons we have used the parameters:

$$a = 0.89, b = 0.18, c = 0.28, k = 0.1$$

When these neuronal maps are coupled to each other by nearest neighbour coupling form, through x, the dynamics of the system is given by [JSGS07]:

$$x_{n+1}(i) = (1 - e)f_1(x_n(i), y_n(i)) + \frac{e}{2}\{g(x_n(i + 1)) + g(x_n(i - 1))\}$$
$$y_{n+1}(i) = f_2(x_n(i), y_n(i)) \tag{2.2}$$

Here, e = coupling strength, n = iteration steps, i = site index on the lattice with periodic boundary conditions.

$g(x)$ is the coupling function and it can take various forms but here we will use, $g(x) = x$.

We simulated the system by taking 100 neurons in the ring

f denotes the initial fraction of active neurons in the ring

Q denotes the fraction of inactive neurons in the ring after simulating the system.

2.2   Results

Effect of coupling strength and the fraction of intrinsically active neurons on neuronal activity is investigated by plotting the fraction of inactive neurons in the ring (Q) with respect to the coupling strength.

Figure 2.1: Q (final fraction of inactive neurons) vs Coupling Strength (e) for different fractions (f) of active neurons in the ring.

Different colors represent different fractions (f) of active neurons in the ring.

Here neural network converges at Q=1 (inactive state) at some critical values of coupling strength (e) for different fractions of active neurons in the ring which are arranged randomly. As the fraction of active neurons increases in the ring, the critical value of coupling strength at which the network converges at the inactive state (Q = 1), also increases.

For each fraction of active neurons in the ring, the critical value of coupling strength at which Q first became 1 is recorded and then plotted w.r.t. f on the graph as shown in Figure 2.2.
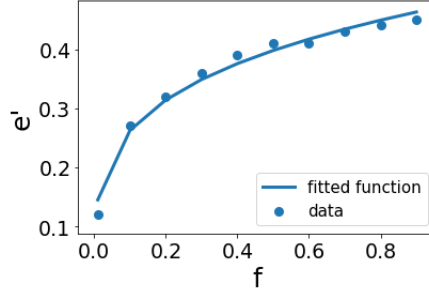
Figure 2.2: e' (critical value of coupling strength at which Q first became 1) vs f (initial fraction of active neurons)

The data fits with the following power law:

$$e' = 0.48f^{0.26} \tag{2.3}$$

Hence, it is observed that for different fractions of active neurons in the ring, all the neurons eventually go to the inactive state (Q = 1) at a particular value of coupling strength. The critical value of coupling strength at which Q first becomes 1 (e') increases as the fraction of active neurons (f) increases as the power law.
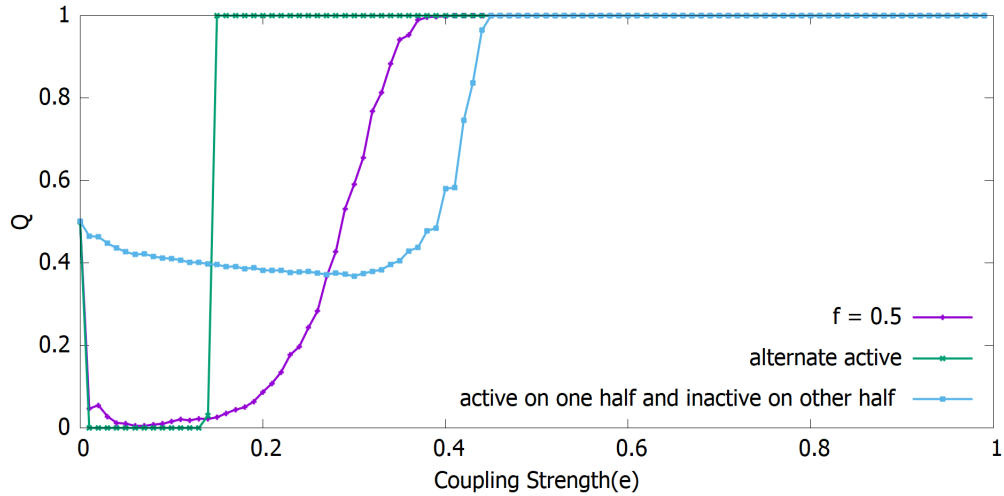
Figure 2.3: Q vs Coupling Strength (e) for three different arrangements of neurons : alternate active, active on one half of the ring and inactive on the other half and 0.5 fraction of active neurons arranged randomly.

Here, the response of the system is compared for three different arrangements of neurons where each arrangement has the same fraction of active neurons. First, active and inactive neurons are

arranged alternatively in the ring. Second, on one half of the ring, there are active neurons while on the other half there are inactive neurons while third is the random arrangement of the neurons in the ring where half of them are active.

In the alternate arrangement of active and inactive neurons, it can be seen that first there is a dip in the graph where all neurons become active (Q=0), after which they eventually converge to the inactive state (Q=1), i.e. there is a window of complete activity. However, the results differ as the arrangement of neurons in the ring is changed, even if the fraction of active neurons is kept the same as shown in Figure 2.3. In all three different arrangements of neurons, alternate active, active on one half of the ring and inactive on the other half and randomly arranged active neurons in the ring, the fraction of active neurons is half but due to their different arrangement, they converge to the inactive state(Q=1) at different values of coupling strength. Their path to the inactive state is also different as there is a clean dip at Q= 0 when active and inactive neurons are arranged alternatively whereas it is not the case in the other two arrangements.
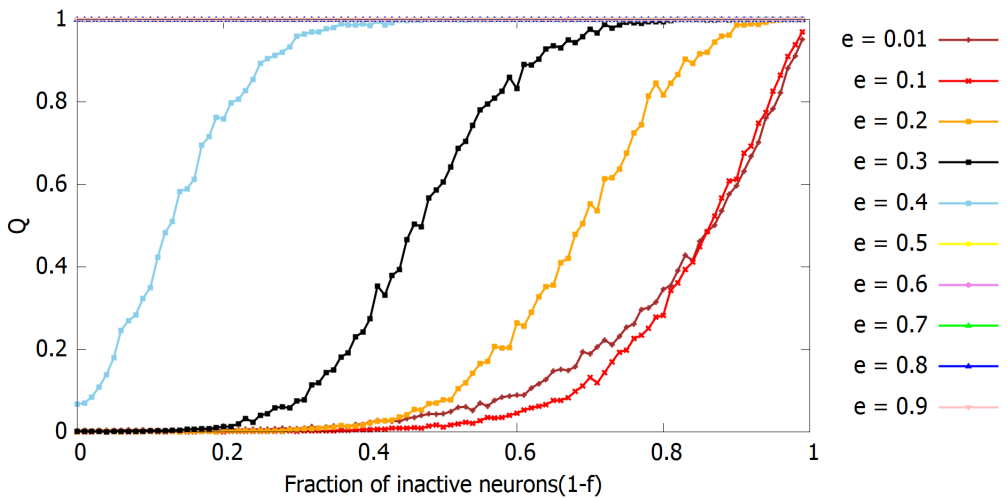
Figure 2.4:   Q vs Initial fraction of inactive neurons (1-f) for different values of coupling strength. Above coupling strength, $e = 0.4$, Q= 1 regardless of the initial fraction of inactive neurons in the ring.

The fraction of inactive neurons (Q) increases monotonically with the initial fraction of inactive neurons in the ring, up to coupling strength 0.4 (Figure 2.4) while at higher coupling strengths($e >$ 0.4), Q becomes 1, independent of the initial fraction of inactive neurons.

2.3   Effect of the size on the dynamics of the network

To check the size dependence on the dynamics of the system, a ring of different size, that is 16 neurons is simulated where each neuron is modeled by the Chialvo map. When these neuronal maps are coupled to each other by nearest neighbour coupling form, through x, the dynamics of the system

is given by:

$$x_{n+1}(i) = (1 - e)f_1(x_n(i), y_n(i)) + \frac{e}{2}\{g(x_n(i + 1)) + g(x_n(i - 1))\}$$

$$y_{n+1}(i) = f_2(x_n(i), y_n(i))$$

(2.4)

The effect of coupling strength and the initial fraction of active neurons on neuronal activity is investigated for the ring of 16 neurons.
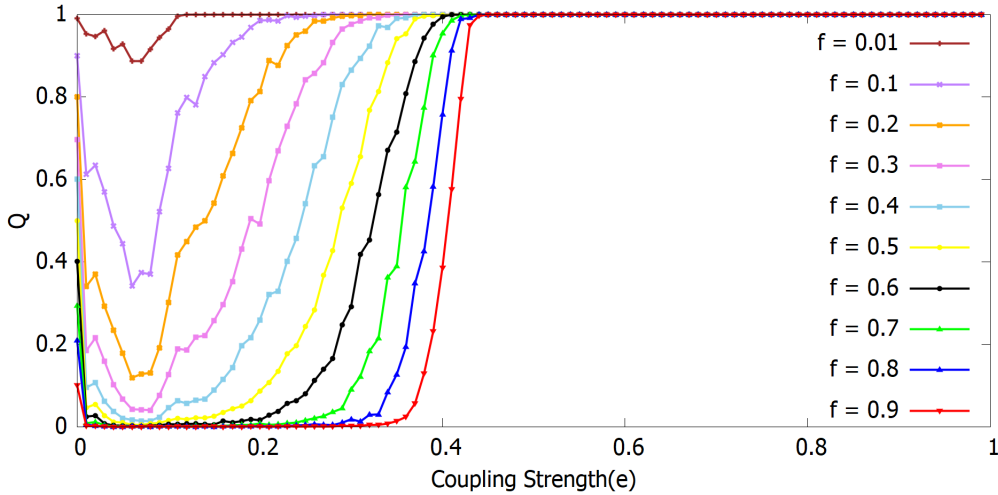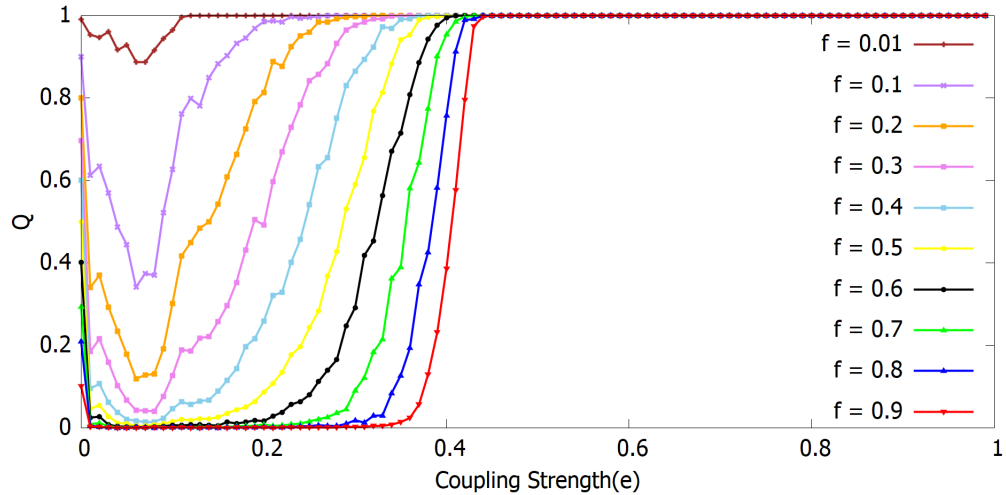

Figure 2.5: Q (final fraction of inactive neurons) vs Coupling Strength (e) for different initial fractions of active neurons in the ring.

Here, different colors represent different initial fractions (f) of active neurons in the ring.

As observed in the case of the ring of 100 neurons, for this case also where there are 16 neurons in the ring, the neural network converges at Q = 1, that is, to the inactive state at certain values of coupling strength (e) for different fractions of randomly arranged active neurons in the ring. Similarly, as the initial fraction of active neurons is increased in the ring, the value of coupling strength at which the network converges at the inactive state (Q = 1), also increases.
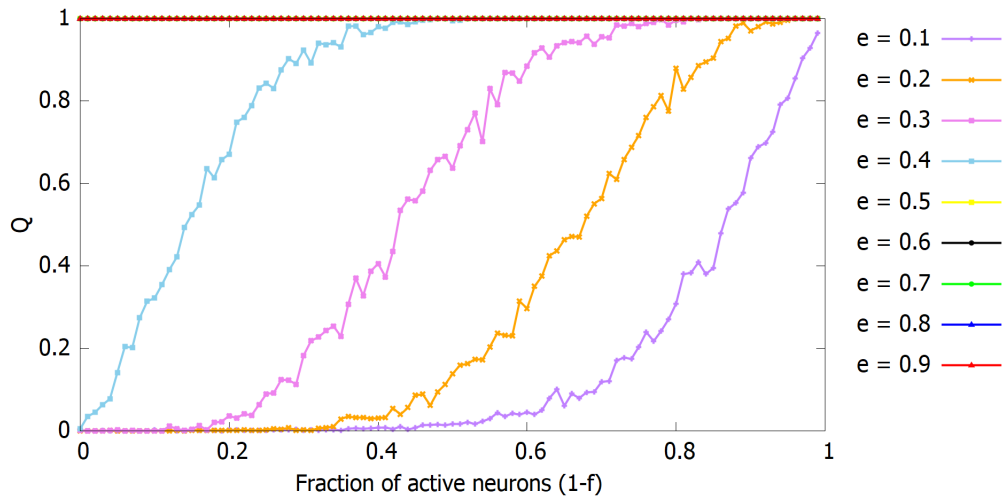
Figure 2.6: Q vs Initial fraction of inactive neurons (1-f) for different values of coupling strength.

As in the case of the ring of 100 neurons, here also, above coupling strength, $e = 0.4$, Q= 1 regardless of the initial fraction of inactive neurons in the ring.

So, it can be concluded that irrespective of the size of the system we get similar collective behavior in the nearest neighbor coupling of neurons, arranged in the ring randomly. The neural network converges to the inactive state at critical values of the coupling strength depending on the initial fraction of active neurons in the network.

Hence, neurons displaying collective dynamics, converge to the inactive state for the nearest neighbor coupling which is independent of the size of the system.

Chapter 3

Neuronal network with mean-field coupling

In chapter 2, the neurons were coupled to each other by nearest-neighbor coupling and it was observed that all neurons ultimately became inactive at a critical value of coupling strength. To understand how the dynamics of the system would change, if neurons were to be coupled by mean-field, the equation determining the dynamics of the system is changed and the response of the system is observed.

3.1   Model

Each neuron in the system is modeled by the two-dimensional Chialvo map[Chi95]. This map will determine the local dynamics of our system. It is defined as:

$$
\begin{aligned}
x_{n+1} &= f_1(x_n, y_n) = x_n^2 exp(y_n - x_n) + k \\
y_{n+1} &= f_2(x_n, y_n) = ay_n - bx_n + c
\end{aligned}
\tag{3.1}
$$

x_n denotes the activation variable and y_n denotes recovery variable in the context of the biological systems.

Parameters k and c are offsets to the variables x_n and y_n while a is rate constant for y_n and b is the activation dependence of the recovery variable as it relates y_n to x_n.

For active state of neurons we have used the parameters:

$$a = 0.89, b = 0.18, c = 0.28, k = 0.04$$

For inactive state of neurons we have used the parameters:

$$a = 0.89, b = 0.18, c = 0.28, k = 0.1$$

The corresponding dynamics of the system is given by:

$$x_{n+1}(i) = f_1(x_n(i), y_n(i)) + e(\bar{x}_n - x_n(i))$$
$$y_{n+1}(i) = f_2(x_n(i), y_n(i))$$

(3.2)

Here, e = coupling strength, n = iteration steps and i = index denoting the ith neuron.

A group of 100 neurons is simulated where the neurons which may be intrinsically active or inactive, are coupled to each other by mean-field coupling. Now, instead of nearest-neighbor coupling, each neuron is coupled to every other neuron in the system.

Ultimately, the effect of active neurons is studied on the collective dynamics of the system, as a function of coupling strength and the fraction of intrinsically active neurons.

3.2 Results
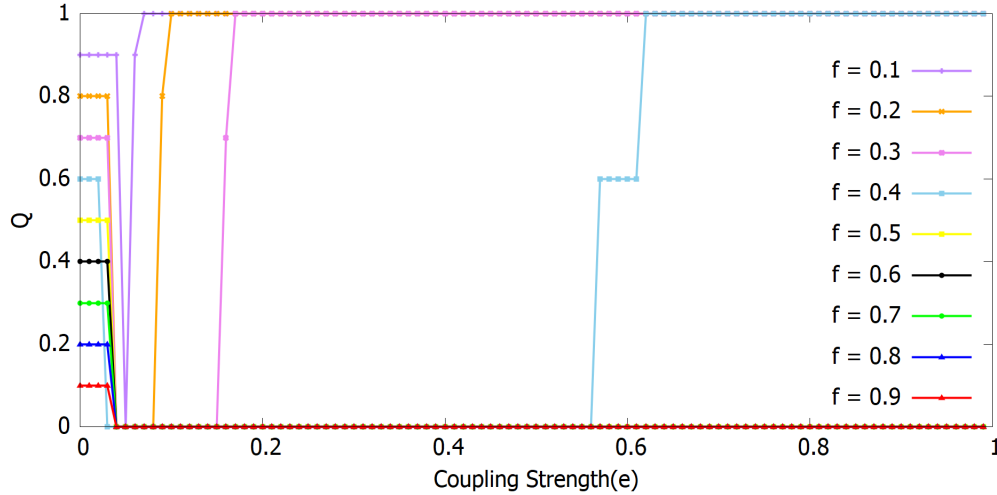
Figure 3.1: Q vs Coupling Strength (e) for different fractions (f) of intrinsically active neurons in the system

In figure 3.1, colors represent a different initial fraction of active neurons (f) in the system. Q is the final fraction of active neurons in the system after the evolution.

The system converges to the inactive state, which is at Q= 1, before briefly coming to the active state if the fraction of active neurons in the system is less than or equal to 0.4. However, if the fraction of active neurons is more than 0.4, the system evolves to the active state, that is Q=0

3.3 Size dependence

Now, the system size is kept 16 to see if there is any size dependence on the dynamics of the system.
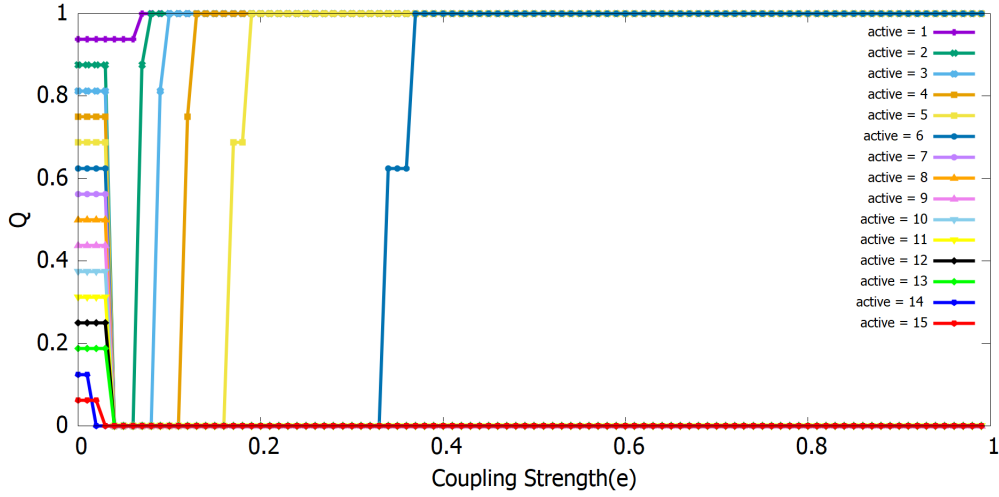
Figure 3.2: Q vs Coupling Strength (e) for different number of intrinsically active neurons in the system

In figure 3.1, colors represent different numbers of initial active neurons in the system.

Here, the number of active neurons is increased one by one to see when does the system exactly changes its collective dynamics. It is observed that in this case also if the fraction of active neurons in the system is less than or equal to 0.4, it ultimately goes to the inactive state. However, if the fraction of active neurons is greater than 0.4, the system evolves to the active state. Hence changing the size of the system does not change the results.

It can be concluded that irrespective of the size of the system when neurons are coupled to each other by mean-field coupling, they display some collective dynamics depending on the initial fraction of active neurons in the system. The system goes to the inactive state ultimately if the initial fraction of active neurons in the system is less than or equal to 0.4 which is termed as the critical fraction. However, there is a window of coupling strength where the system becomes active before going to the inactive state. This width of the window where the system becomes active increases as the fraction of active neurons is increased. While the system goes to the active state if the initial fraction of active neurons in the system is kept more than 0.4. It can be concluded that this critical fraction of active neurons which determines the change in the collective dynamics of the system remains constant even if the size of the system is changed.

Chapter 4

Effect of active oscillators in the coupled MBH system

The mercury beating heart (MBH) system which is a chemo-mechanical oscillator is not only visually spectacular but also a very simple experiment to perform. The only thing one needs to be careful about is the handling of mercury which is toxic. It can be used to observe the various phenomena exhibited by coupled oscillators. Here, it is used to see the effect of an active oscillator on the globally coupled oscillators.

4.1   Mechanism of an autonomous MBH oscillator

When charges accumulate on the mercury surface due to its oxidation in the presence of the oxidizing agent, there is an electric repulsion among the like charges which leads to the decrease in the surface tension. Due to the decreased surface tension, mercury drop flattens and as it expands, its surface area increases. As the iron nail is touched to the mercury surface, the mercury surface gets discharged due to its reduction by iron, and Hg again contracts to its original state as the surface tension increases. This charging and discharging and change in the surface tension leads to change in the surface area of the mercury drop as it expands and contracts[Avn89]. The redox reactions occurring in the system and the change in surface tension leads to contraction and relaxation of the mercury surface like a heart, which we term as an autonomous oscillator.
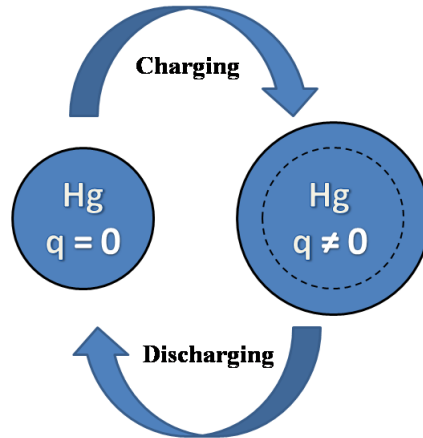
Figure 4.1:   Schematic of charging and discharging of Mercury

4.2   Active and inactive oscillator

Whether the oscillator is autonomous or forced/nonautonomous, it is termed as an active oscillator if it exhibits oscillations. However, if the oscillator shows no oscillations then it is an inactive oscillator.

4.3   Setup

Six mercury oscillators were prepared using 2 ml of Hg, $6MH_2SO_4$, and $6MCe(SO_4)_2$ in different sections of the plastic tray. Each section of the tray had a platinum wire connection at the bottom which was extended through the copper wire to connect it with other oscillators. The wire connected to the Hg should be inert and should not form an amalgam with mercury. Therefore either platinum or tungsten could be used to make the connection with mercury.

All the oscillators were then globally coupled through the resistors of 5 ohms. Each one of the oscillators was connected to every other oscillator through the resistors, such that one end of all the resistors was at one common point and their other end was connected to the individual oscillators. The total resistance between the two oscillators was 10 ohms. The coupled MBH system was then put in the common aqueous medium of sulphuric acid. Iron nails were placed near the oscillators in different sections of the tray. These iron nails were then connected to common ground.
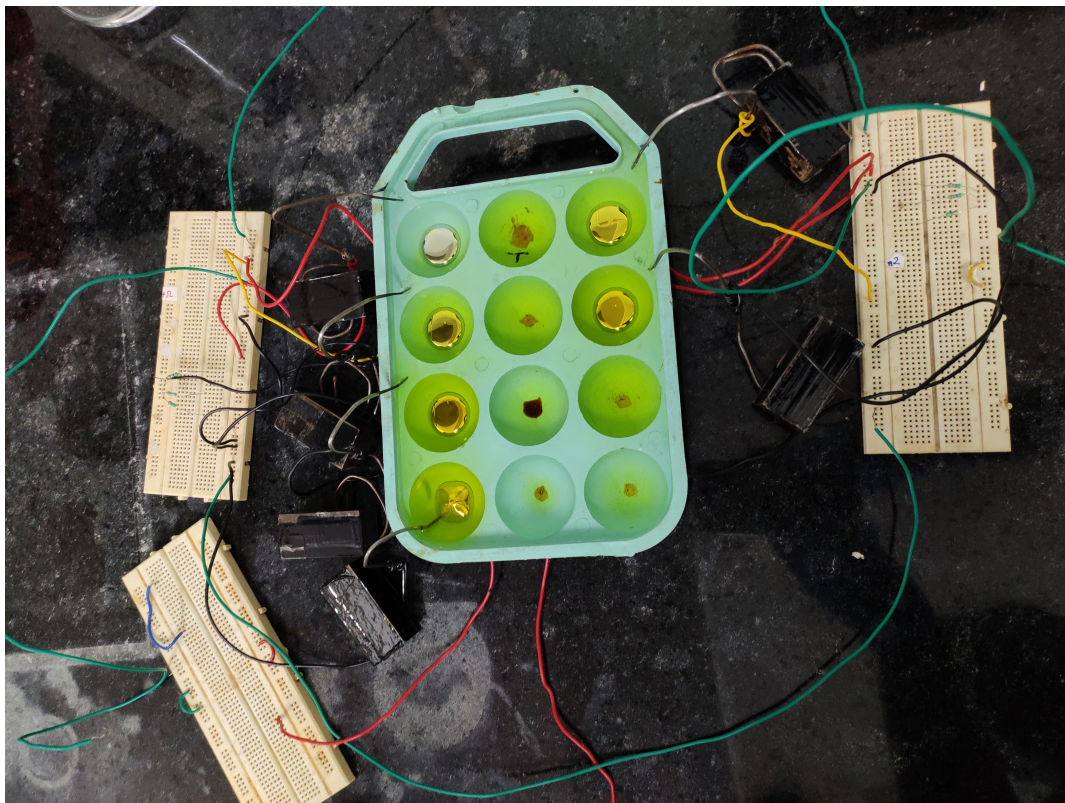
Figure 4.2: Image of the setup.

4.4 Procedure

In the experiment, one of the oscillators was made autonomous, that is a pointed iron nail was just touched to the periphery of the Hg to get self-sustained oscillations. The autonomous oscillator was uncoupled from the system earlier until it gains self-sustained oscillations. Afterward, it was coupled to all the oscillators. The effect of this autonomous oscillator was then observed on the globally coupled system.

4.5 Results

During the oscillations of the MBH system, the electron flow between different chemical species causes oxidation and reduction of mercury which leads to the contraction and expansion of the mercury drop. Figure 4.3 shows a typical time series of the redox potential of the mercury drop. The rising potential corresponds to the oxidation of mercury where charge accumulates on its surface and it leads to an increase in the potential slowly which then reaches a maximum value. When the iron nail touches the periphery of the mercury drop, there is a rapid fall of the potential in the time series. The potential is zero when there is continuous contact between the iron and mercury drop. This cycle continues as mercury oxidizes again and potential rises, reaches the maximum, and drops again as iron reduces the mercury.
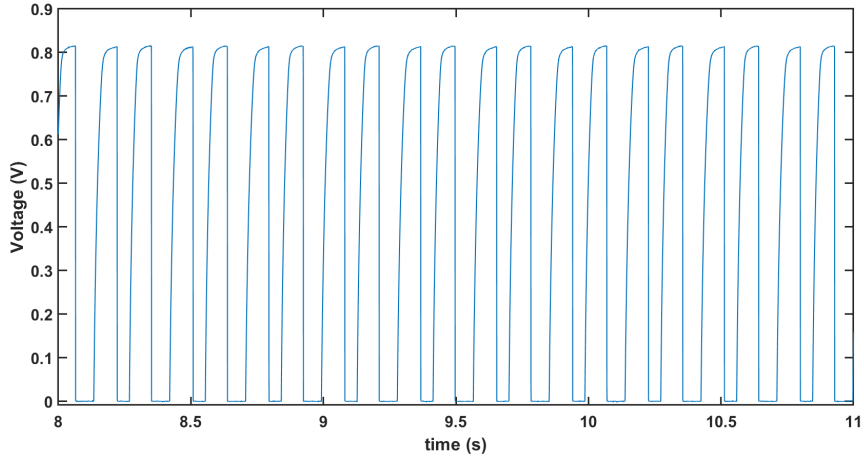
Figure 4.3:   Redox time series of an autonomous oscillator

By recording the video clip of the top view of the mercury drop, the evolution of the area of the mercury drop can be determined. The time evolution of the area of the mercury drop is shown in figure 4.4. When mercury oscillates, there is a change in its radius and thus in its surface area, as it expands and contracts which is shown in part (a) of figure 4.4, we term this oscillator as an active oscillator. Whereas if the area of the mercury drop remains constant with time and there are no oscillations in the MBH system, we term it as an inactive oscillator as shown in part (b) of figure 4.4.
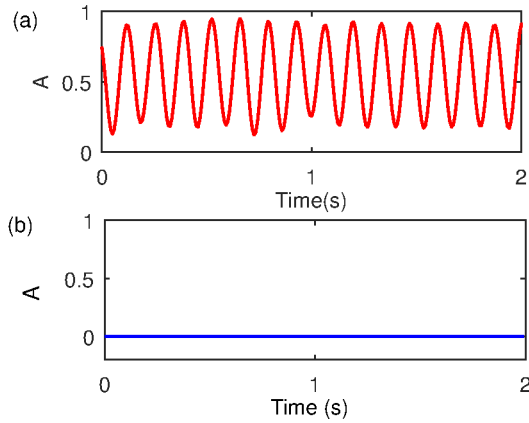
Figure 4.4: Area evolution of an active (a) and an inactive (b) MBH oscillator

The six MBH oscillators were globally coupled to each other through the resistors and one of them was made active which we call as an autonomous oscillator. It was observed that one autonomous oscillator triggered the oscillations in all other oscillators which were earlier inactive. But, since the iron nails were not touching the mercury drops in the case of the rest of 5 MBH oscillators, these oscillators are now forced or non-autonomous oscillators.

The redox time series for the autonomous and one of the nonautonomous oscillators, which were earlier inactive is shown in figure 4.5. It could be seen that the inactive oscillator has become active and the phases of both the oscillators have synchronized.

As can be seen in figure 4.5, the potential of the autonomous one however completely comes to zero as the mercury drop touches the iron nail, but for the nonautonomous one, the potential does not go to zero.
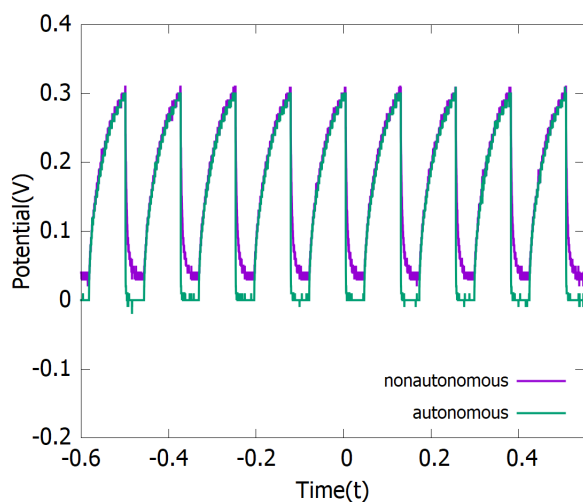
Figure 4.5: Redox time series of an autonomous oscillator and one of the representative inactive oscillator which became nonautonomous/forced oscillator due to the forcing of the active oscillator.

The redox time series of two nonautonomous oscillators is as shown in figure 4.6. These two also go to the active state and are phase synchronized. As these two are forced oscillators, their phases are the same.
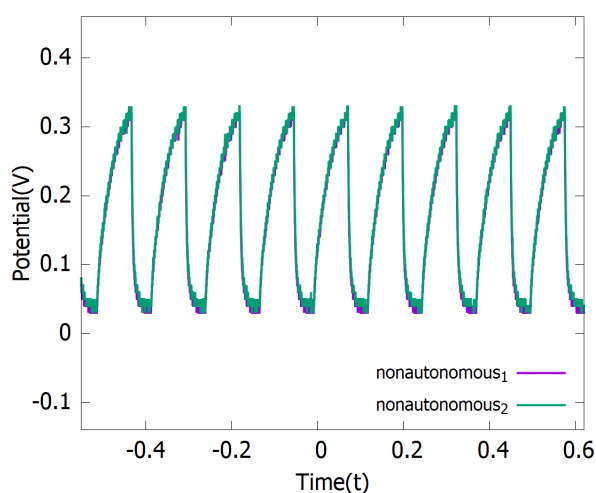
Figure 4.6: Redox time series of two nonautonomous oscillators

It can be concluded that if six MBH oscillators are placed in the common aqueous solution, one autonomous MBH oscillator could trigger oscillations in all other oscillators. All the oscillators would converge to the active state and become phase synchronized. Therefore, one or more than one autonomous oscillators in the system could drive all the globally coupled oscillators to the active state.

4.6 Simulating MBH system using the FHN model

In the MBH system, it is observed that one autonomous oscillator could trigger oscillations in the rest of the oscillators. This system is modeled using the FHN model[Fit61] which is also an example of a relaxation oscillator.

We first try to simulate the experimental results by taking 6 oscillators coupled to each other by mean-field coupling.

The dynamics of the system is given by the equations:

$$\frac{dv_i}{dt} = v_i - \frac{v_i^3}{3} - \omega_i + I_{ext} + e(\bar{v} - v_i)$$
$$\tau \frac{d\omega_i}{dt} = v_i + a - b\omega_i$$

(4.1)

Here e is the coupling strength, v is the membrane potential, ω is the recovery variable, I_{ext} is the external stimulus, and a and b and τ are dimensionless, positive and used for the time scale and kinetics of the recovery variable.

For active state of neurons we have used the parameters:

$$a = 0.7, b = 0.8, \frac{1}{\tau} = 0.08, I_{ext} = 1.0$$

For inactive state of neurons we have used the parameters:

$$a = 0.7, b = 0.8, \frac{1}{\tau} = 0.08, I_{ext} = 0.1$$

This differential equation was solved using the 4th order Runge-Kutta method. Initially, out of six oscillators, one oscillator is selected as an active oscillator and the others are kept inactive. Then, the number of active neurons is increased in the system and the collective dynamics is observed.
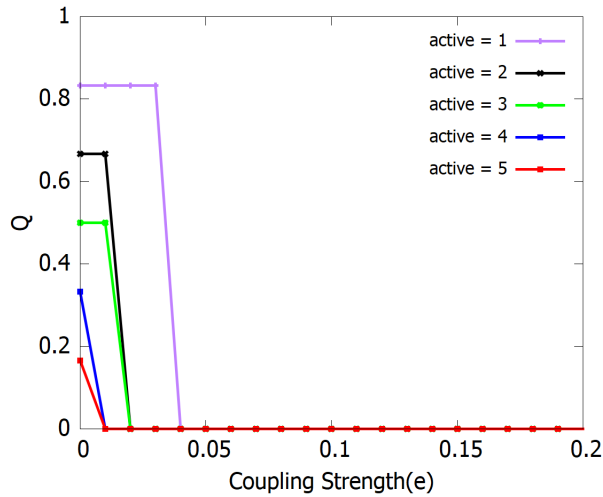
Figure 4.7: Q (final fraction of inactive neurons) vs Coupling Strength (e) for different number of intrinsically active neurons in the system

It can be observed from the figure that one active neuron can drive all other coupled neurons to the active state. As the number of active neurons is increased, the system goes to the active state at much lower coupling strength. Hence the results are the same as we observed in the MBH experiment.

4.7 Size dependence

Now, instead of six neurons,100 neurons are coupled to each by mean-field coupling.
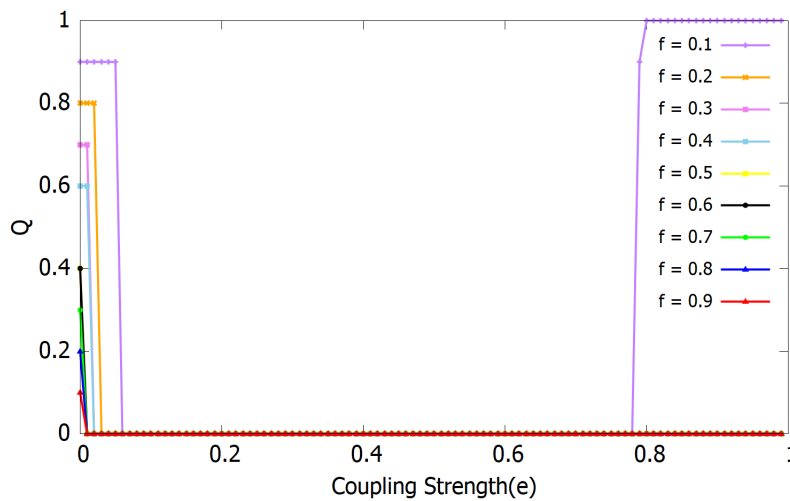
Figure 4.8: Q (final fraction of inactive neurons) vs Coupling Strength(e) for different fractions (f) of intrinsically active neurons in the system

Here, f denotes the initial fraction of active neurons in the system.

As the size of the system is increased, it still goes to the active state, the coupling strength at which the system becomes active decreases as the fraction of active neurons is increased. However, with a very low fraction of active neurons, that is, 0.1, at coupling strength 0.79, Q starts increasing and goes to 1 at $e = 0.8$. The system becomes inactive, that is Q becomes 1, at $e = 0.8$.

In the MBH experiment, we could only do the experiment with six oscillators, and there the minimum fraction of active neurons was $\frac{1}{6}$, which is 0.17. So, we could not verify the collective dynamics of the system for 0.1 fractions of active neurons. It is really very difficult to perform the experiment with 100 oscillators to see whether the same phenomenon will be observed in the experiment. We could, of course, do the experiment with ten oscillators while keeping one oscillator active but due to technical difficulties we could not perform the experiment for more than eight oscillators.

But, we can say that this model is a better fit for the MBH system than the Chialvo map.

From our experiment, it could be concluded that in the MBH system, one oscillator could trigger the oscillations in the whole system. This system was then modeled using the FHN model which gave the same results for the six oscillators as observed in the experiment, that is the all neurons became active. However, for the system size of 100 neurons, it was observed that for the fraction of active neurons less than or equal to 0.1, the system goes to the inactive state at high coupling strength. This observation could not be verified experimentally due to the technical difficulties but it could be said that the FHN model is the better fit to model the MBH system than the Chialvo map. However, for the fraction of active neurons greater than 0.1, the system goes to the active state. This result is similar to the Chialvo map result where neurons were coupled to each other by mean-field coupling in the sense that there was a critical value of the fraction of active neurons (f = 0.4) in the system above which only the system goes to the active state. But, the FHN model gives us the results closer to our experiment. That's why it is a better fit.

Chapter 5

Emergent patterns in two coupled neuronal sub-populations.

Emergent phenomena have earlier been studied in two interacting populations of model neurons where the interacting populations are in different dynamical domains[KS15]. The idea behind studying such a system is that our brain is composed of neurons and the interacting neuronal groups could be in different dynamical domains. Here, we consider two interacting sub-populations of model neurons where the local dynamics of these neurons is determined by the FHN model. The neurons in each sub-population can be active or inactive depending on the parameters of the governing differential equations. We try to study how one group influences the dynamics of the other as a function of coupling strength, connection density, and population size.

5.1 Model

The local dynamics of the system is determined using the FHN model. We consider a network of neurons where each node denotes our model neuron whose dynamics is determined by a set of differential equations given below:

$$
\begin{aligned}
\frac{dv_i}{dt} &= v_i - \frac{v_i{}^3}{3} - \omega_i + I_{ext} \\
\tau \frac{d\omega_i}{dt} &= v_i + a - b\omega_i
\end{aligned}
\tag{5.1}
$$

Here v is the membrane potential, ω is the recovery variable, I_{ext} is the external stimulus, and a and b and τ are dimensionless, positive parameters and used for the time scale and kinetics of the recovery variable.

Now, we consider two sub-populations denoted by A and B. The neurons in sub-population A are active while in sub-population B are inactive. The intra-group and inter-group coupling strengths are e_1 and e_2 respectively. The dynamics of the interactive sub-populations A and B is governed by the following equations :

$$\frac{dv_A^i}{dt} = v_A^i - \frac{{v_A^i}^3}{3} - w_A^i + I_A + e_1(\bar{v}_A - v_A^i) + \sum_{j=1}^{c} A[i,j]\frac{e_2}{c}(v_B^j - v_A^i)$$

$$\frac{d\omega_A^i}{dt} = \frac{1}{\tau}(v_A^i + a - b\omega_A^i)$$

$$\frac{dv_B^i}{dt} = v_B^i - \frac{{v_B^i}^3}{3} - w_B^i + I_B + e_1(\bar{v}_B - v_B^i) + \sum_{j=1}^{c} B[i,j]\frac{e_2}{c}(v_A^j - v_B^i)$$

$$\frac{d\omega_B^i}{dt} = \frac{1}{\tau}(v_B^i + a - b\omega_B^i)$$

Here, c = number of connections of an individual neuron in the other sub-population. The value of parameters used are: $a = 0.7, b = 0.8, \frac{1}{\tau} = 0.08, I_A = 1.0, I_B = 2.0$ and e_1 i.e. the intra-group coupling is kept constant at 0.5.

We consider a unidirectional inter-group coupling here. A and B matrices are formed based on connection probability, for example, for connection probability (ρ) = 0.1, we select a random number, r between 0 and 1. If r < 0.1 then we put A [i, j] = 1. Now, these equations are solved using RK4 by taking dt = 0.01. After leaving (1000/dt) transients, we evolve the system for (500/dt) steps and record the time series of each neuron of both the sub-populations. We find the amplitude (i.e. [global maxima - global minima] of the time series) of each neuron of a sub-population and see that the amplitude of each neuron in a sub-population comes out to be almost same for a set of parameters. So, we average over all the amplitudes to find the averaged amplitude of a sub-population.

5.2   Results for population size (50,3)

In sub-population A there are 50 active neurons while in sub-population B there are 3 inactive neurons. Now the inter-group coupling (e_2) and the connection probability (ρ) are varied with a step of 0.01 and averaged amplitude is recorded for each sub-population.

(a) sub-population A
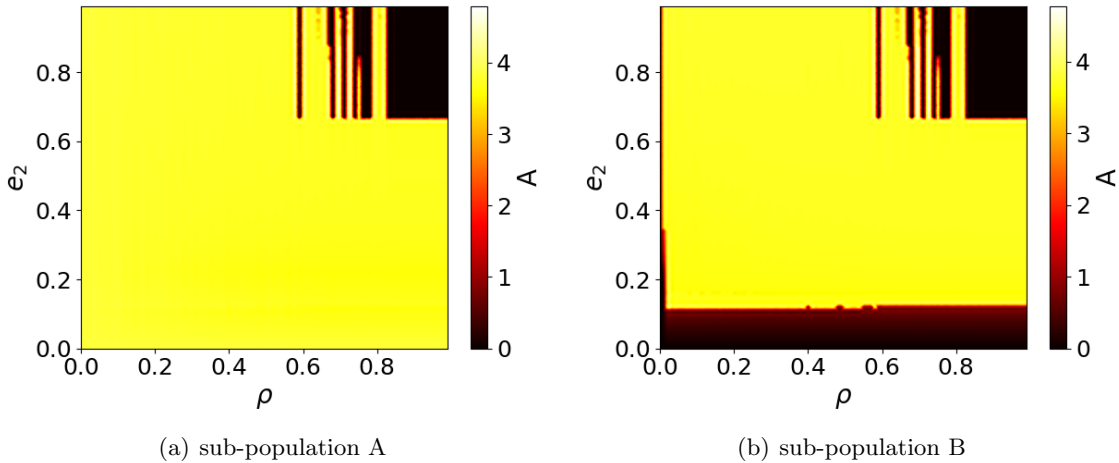
(b) sub-population B

Figure 5.1: Variation of the amplitude of each sub-population w.r.t. e_2 and ρ for population size (50,3)

28

It could be seen that within the active sub-population A the amplitude starts decreasing at moderate values of ρ and higher values of e_2. As the value of ρ is further increased, the window of amplitude death becomes wider at relatively lower values of e_2. Thus, increasing the number of connections between the two sub-populations aids the amplitude death. While in the inactive sub-population B, the group is inactive at less number of connections, but as the connection probability is increased, the sub-population becomes active in a region of moderate ρ and e_2. As the connection probability is increased beyond 0.6, the amplitude starts decreasing at higher inter-group coupling strength. Amplitude death is aided by increasing ρ and as the ρ is increased, the amplitude death occurred at relatively low values of e_2.

Therefore, even if there are more active neurons (50) in sub-population A than inactive (3) neurons in sub-population B, both populations go to inactive state at high values of ρ and e_2.

(a) sub-population A   (b) sub-population B

Figure 5.2: Effect of rewiring of connections on amplitude variation of each sub-population w.r.t. e_2 and ρ for population size (50,3)

Now the connections are rewired after every 10 dynamical updates (i.e. at t =0.1, starting from t =0, with dt =0.01) in both populations.

Rewiring the connections doesn't have much effect on amplitude death. The rewired connections, however, give a smooth transition to the amplitude death window in both populations.

(a) sub-population A   (b) sub-population B
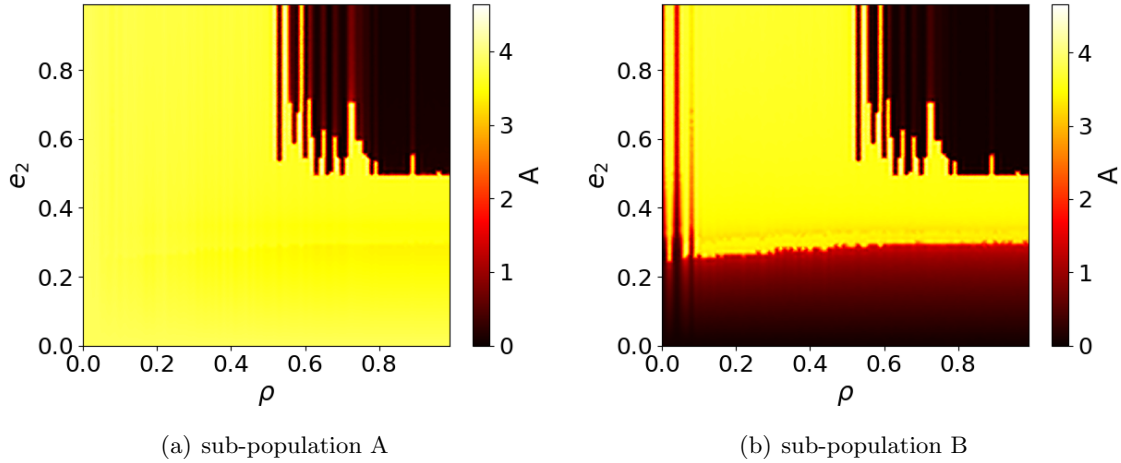
Figure 5.3: Variation of the amplitude w.r.t. e_2 and ρ for each sub-population of population size (50,3) where external impulses are randomly distributed

Now, I_1 and I_2 are randomly distributed over a range of values rather than keeping them constant. I_1 is kept in the range; [0.4,1.4] where neurons are active while I_2 lies in the range; [2,3] where neurons are inactive.

Uniform random distribution of the external impulse gives a larger window of amplitude death. The window of amplitude death occurs at relatively moderate values of ρ and e_2.

(a) sub-population A   (b) sub-population B
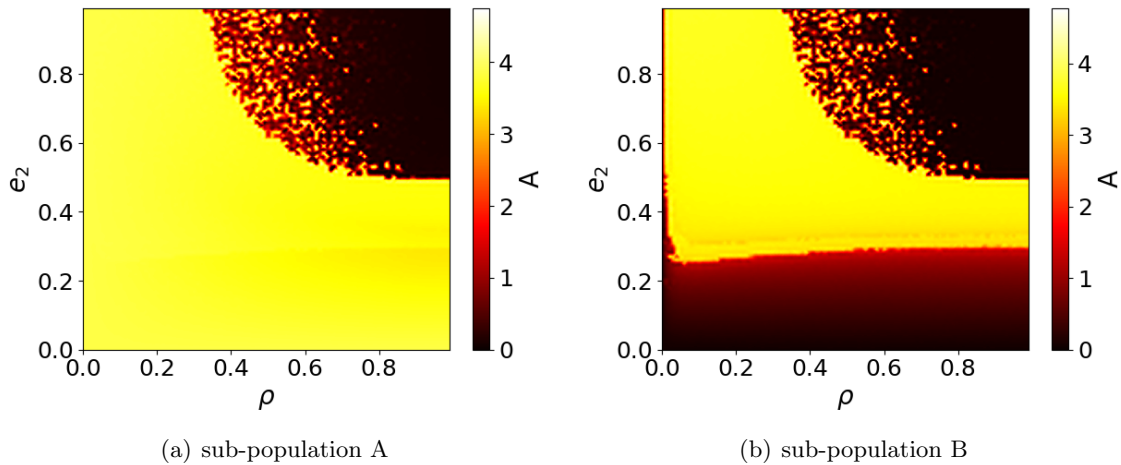
Figure 5.4: Variation of the amplitude of each sub-population for population size (50,3) w.r.t. e_2 and ρ where connections are rewired while randomly distributing the external impulses

Now, the connections are rewired after 10 dynamical updates while taking random uniform distributions of I_1 and I_2 over the above-defined range.

Rewiring the connections gives smoother boundaries on the transition of populations to the inactive state.

Hence, in the population size (50,3), high values of ρ aided the amplitude death and made the window wider. As ρ is increased in the window of amplitude death, the value of e_2 at which amplitude death occurred decreases.

5.3   Results for population size (3,50)

In sub-population A there are 3 active neurons while in sub-population B there are 50 inactive neurons. Now the inter-group coupling (e_2) and connection probability (ρ) are varied with a step of 0.01 and averaged amplitude is recorded for each sub-population.

(a) sub-population A   (b) sub-population B
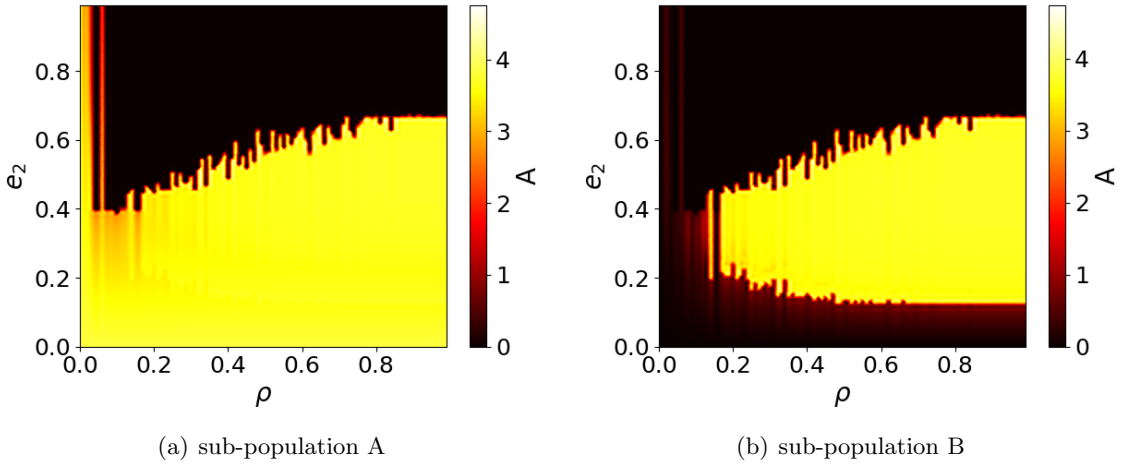
Figure 5.5: Variation of the amplitude of each sub-population w.r.t. e_2 and ρ for population size (3,50)

There is amplitude death even at very low ρ and moderate e_2 for sub-population A. However, the window of amplitude death shrinks as the connections and coupling strength are increased but ultimately the population becomes inactive even at higher connection probability and coupling strength.

Since the size of inactive sub-population B is very large as compared to active sub-population A, at low values of ρ and e_2 the sub-population B remains inactive, but as the connections are increased there is a window where all neurons become active between low to moderate coupling strength. However, at higher coupling strengths, the population B remains inactive but more number of connections suppressed the amplitude death window.
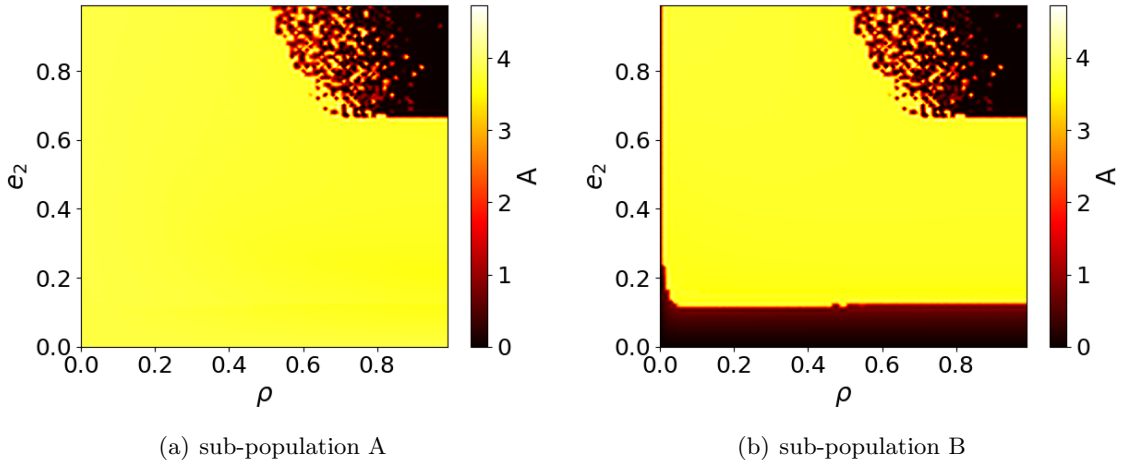
(a) sub-population A
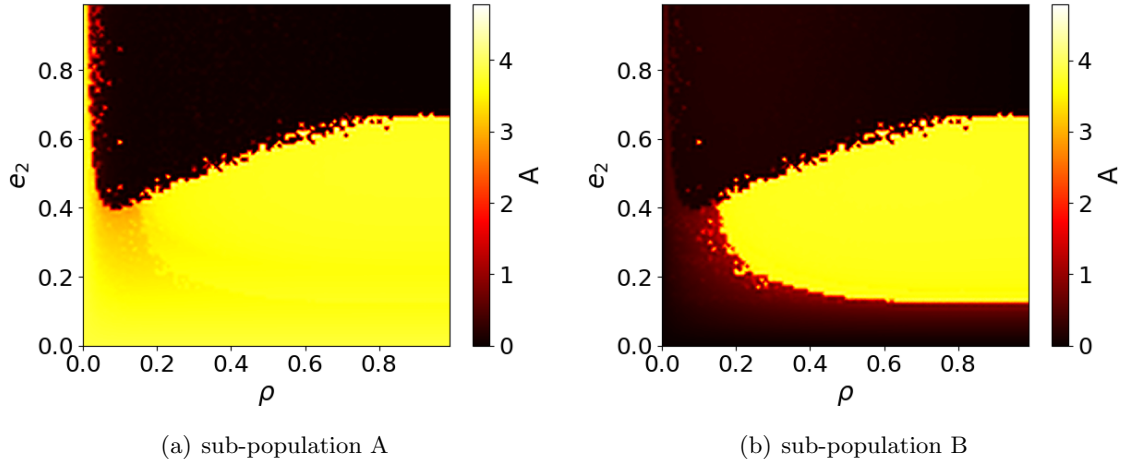
(b) sub-population B

Figure 5.6: Effect of rewiring of connections on amplitude variation of each sub-population w.r.t. e_2 and ρ for population size (3,50)

Now the connections are rewired after every 10 dynamical updates (i.e. at t =0.1, starting from t =0, with dt =0.01) in both populations.

Rewiring the connections doesn't have much effect on amplitude death. The rewired connections, however, give a smooth transition to the amplitude death window in both populations.

(a) sub-population A
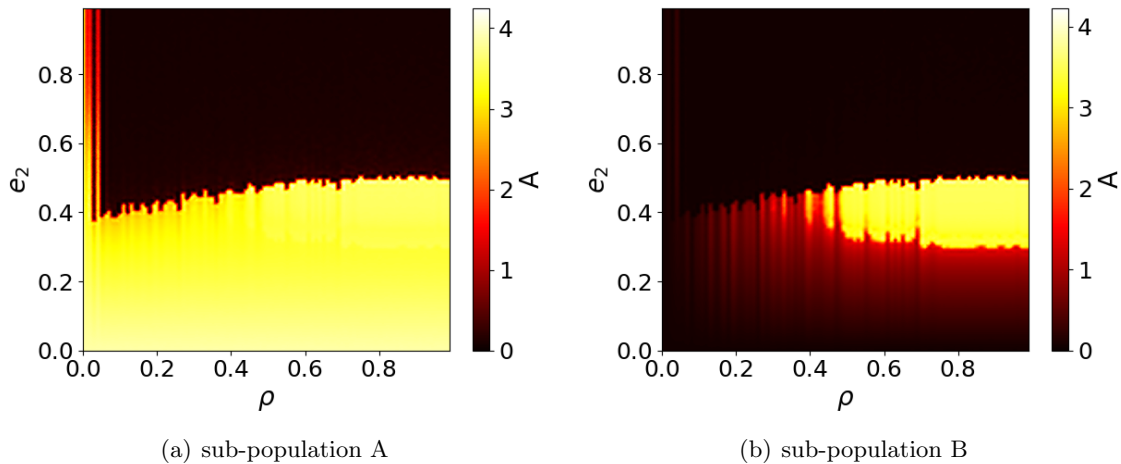
(b) sub-population B

Figure 5.7: Variation of the amplitude w.r.t. e_2 and ρ for each sub-population of population size (3,50) where external impulses are randomly distributed

Now, I_1 and I_2 are randomly distributed over a range of values rather than keeping them constant. I_1 is kept in the range; [0.4,1.4] where neurons are active while I_2 lies in the range; [2,3] where neurons are inactive.

Uniform random distribution of the external impulse gives a larger window of amplitude death. The window of amplitude death occurs at relatively moderate values of ρ and e_2 and the active window where all neurons are active shrinks in both populations.

(a) sub-population A
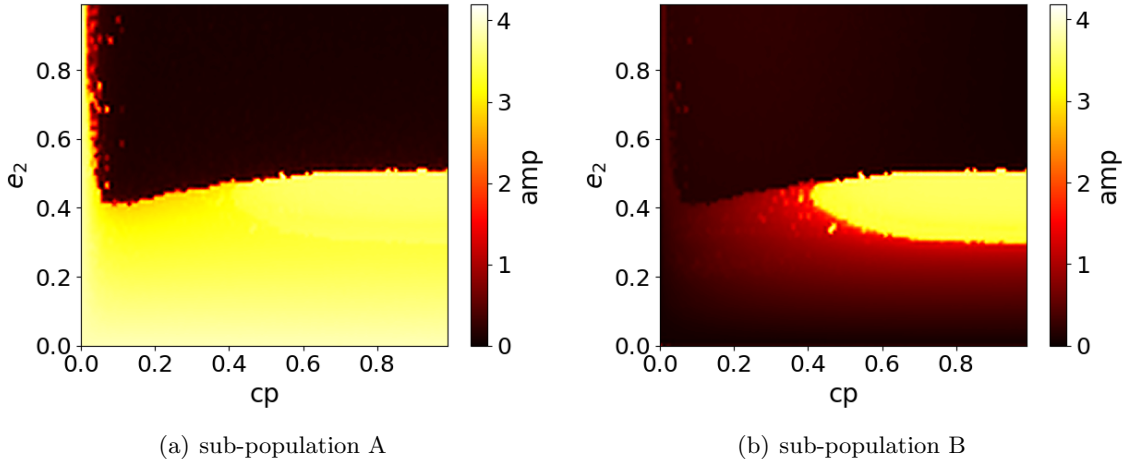
(b) sub-population B

Figure 5.8: Variation of the amplitude of each sub-population for population size (3,50) w.r.t. e_2 and ρ where connections are rewired while randomly distributing the external impulse

Now, the connections are rewired after 10 dynamical updates while taking random uniform distributions of I_1 and I_2 over the above-defined range.

Rewiring the connections gives smoother boundaries on the transition of populations to the inactive state.

Hence, in the population size (3,50), high values of ρ suppressed the amplitude death and made the window narrower. As ρ is increased in the window of amplitude death, the value of e_2 at which amplitude death occurred increases.

5.4 Results for population size (10,16)

In sub-population A there are 10 active neurons while in sub-population B there are 16 inactive neurons. Now the inter-group coupling (e_2) and connection probability (ρ) are varied with a step of 0.01 and averaged amplitude is recorded for each sub-populations.

(a) sub-population A   (b) sub-population B
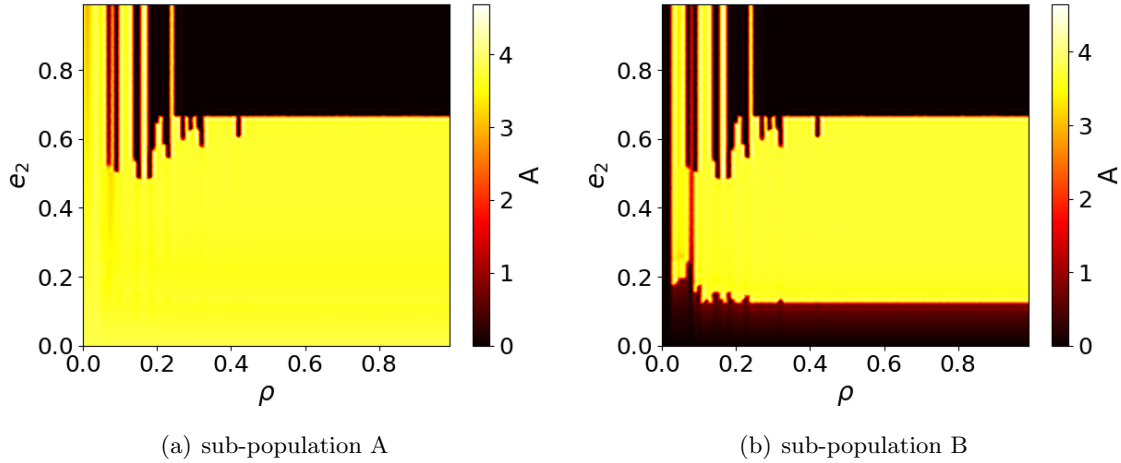
Figure 5.9: Variation of the amplitude of each sub-population w.r.t. e_2 and ρ for population size (10,16)

In sub-population A, amplitude death occurred in the window of moderate e_2, i.e. around 0.6 and low ρ. The active sub-population undergoes amplitude death over moderate inter-group coupling strength and remain inactive at high ρ and e_2.

While in sub-population B, already inactive neurons remain inactive at low and above moderate values of e_2. However, there is an active window in between where all neurons become active.

(a) sub-population A   (b) sub-population B
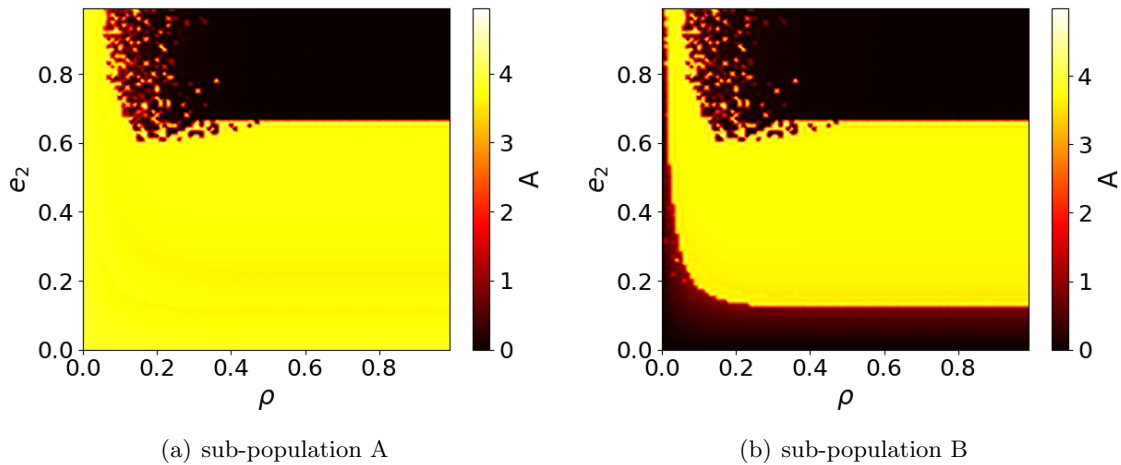
Figure 5.10: Effect of rewiring of connections on amplitude variation of each sub-population w.r.t. e_2 and ρ for population size (10,16)

Now the connections are rewired after every 10 dynamical updates (i.e. at t =0.1, starting from t =0, with dt =0.01) in both populations.

Rewiring the connections doesn't have much effect on amplitude death. The rewired connections, however, give a smooth transition to amplitude death in both populations.

(a) sub-population A   (b) sub-population B
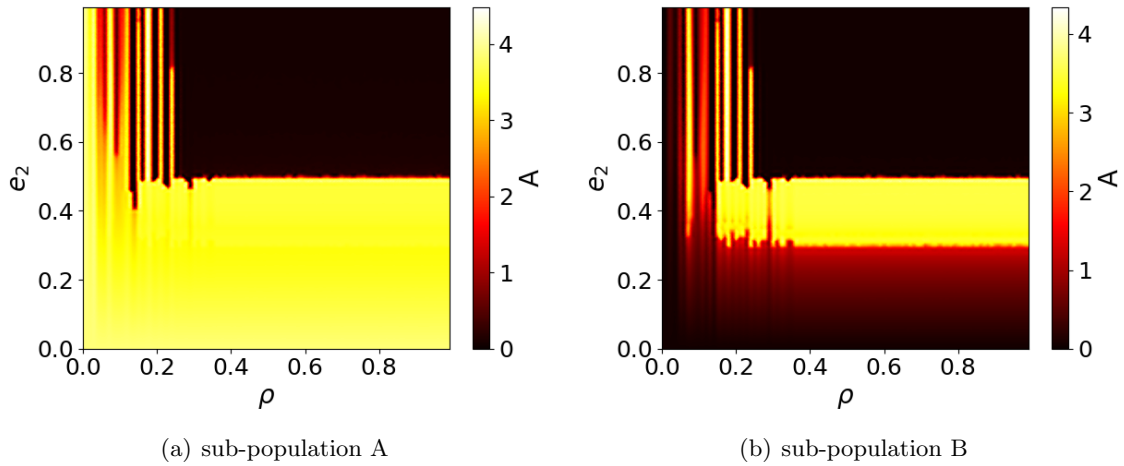
Figure 5.11: Variation of the amplitude w.r.t. e_2 and ρ for each sub-population of population size (10,16) where external impulses are randomly distributed

Now, I_1 and I_2 are randomly distributed over a range of values rather than keeping them constant. I_1 is kept in the range; [0.4,1.4] where neurons are active while I_2 lies in the range; [2,3] where neurons are inactive.

Random distribution of external impulse over a range of values makes the amplitude death window wider. Amplitude death occurred at relatively low values of inter-group coupling strength in sub-population A.The active window in sub-population B became narrower and the two windows of amplitude death widened.

(a) sub-population A   (b) sub-population B
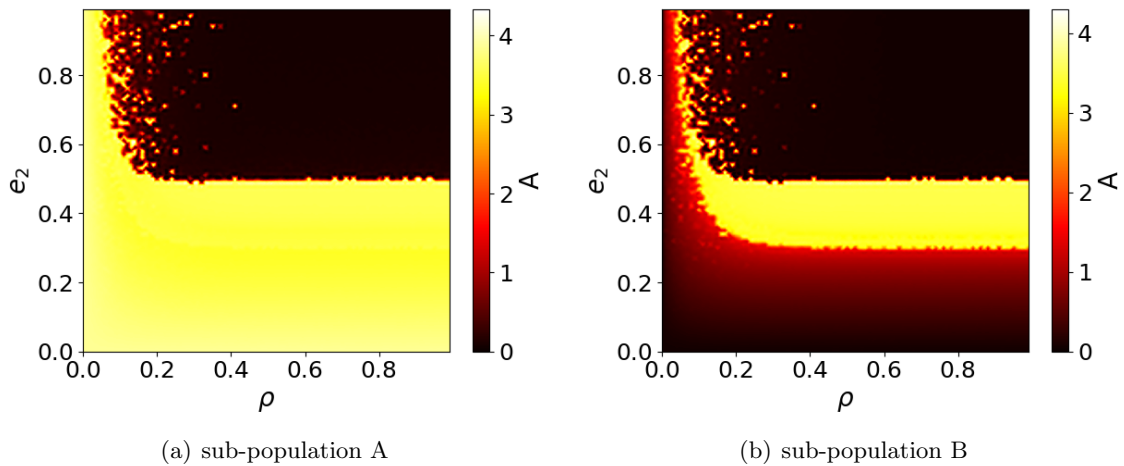
Figure 5.12: Variation of the amplitude of each sub-population for population size (10,16) w.r.t. e_2 and ρ where connections are rewired while randomly distributing the external impulse

Now, the connections are rewired after 10 dynamical updates while taking random uniform distributions of I_1 and I_2 over the above-defined range.

Rewiring the connections gives smoother boundaries on the transition of populations from the active state to the inactive state and vice versa.

Therefore, it could be concluded that the amplitude death window occurred in all three population sizes independent of the size of active sub-population.In the population sizes (3,50) and (10,16) inactive sub-population sizes were larger and amplitude death occurred above intermediate values of inter-group coupling strength and at low values of ρ.

While in the population size (50,3), despite the large size of active sub-population, counter-intuitively there is still an amplitude death window at relatively high values of connection probability. The population goes to the inactive state instead of the active state, the only difference is that the amplitude death window is smaller and occurred at a higher ρ than the other two cases. Rewiring of connections doesn't have much effect on the amplitude death window, however, it gives smoother boundaries at the transition of sub-populations from one state to another. Uniform random distribution of external impulse over a range of values makes the amplitude death window wider. Increasing the number of connections between the two sub-populations aids the behavior of the smaller sub-population i.e. if there are less active neurons then the amplitude death window will shrink and if there are less inactive neurons then the amplitude death window becomes wider.

Chapter 6

Conclusion and Future Work

6.1 Concluding remarks

In this thesis, the effect of active neurons is studied in a network of coupled neurons where each neuron is modeled using discrete and continuous-time units. First of all, a ring of neurons was coupled to their nearest neighbors where the Chialvo map was considered as the local dynamical unit. It was observed that for different fractions of active neurons in the ring, all neurons eventually go to an inactive state at a critical value of coupling strength. However, for the mean-field coupling, the system goes to the inactive state if the fraction of active neurons is less than or equal to the critical fraction i.e. 0.4. Whereas the system goes to the active state if the fraction of active neurons in the system is kept more than the critical fraction. In both nearest neighbor and mean-field coupling cases, the results are independent of the size of the system and the critical value of coupling strengths and active fractions in the system remain constant even if the size of the system is changed.

Then experiments were performed to see the effect of the active oscillator in a globally coupled MBH system and it was observed that one or more than one autonomous MBH oscillator could trigger oscillations in all other oscillators. All six oscillators go to the active state and become phase synchronized. This system was then simulated by taking a continuous-time FHN model where a group of neurons was coupled by mean-field coupling. It showed similar results as of the experiment for the six oscillators but a slight deviation for larger system sizes. It was observed that for the fraction of active neurons less than or equal to 0.1, (which is similar to the critical fraction of Chialvo map in the mean-field coupling case) the system goes to the inactive state at high coupling strength which could not be verified by experiment due to the technical difficulties. The FHN model gave the results similar to the experiment hence was a better fit than the Chialvo map for the MBH coupled system. Lastly, two interacting sub-populations of model neurons where the local dynamics of these neurons is determined by the FHN model were considered in different dynamical domains. One sub-population was considered active while other was considered inactive and the effect of population size, inter-group coupling strength, rewiring of connections, and the number of connections was observed. Amplitude death occurred in all three population sizes, (50,3),(3,50), and (10,16). In population sizes where inactive sub-population was larger, amplitude death occurred at low ρ while in population size where active sub-population was larger amplitude death occurred at higher values of ρ. As the number of connections is increased, the behavior of smaller sub-population persists. If the smaller sub-population is active, amplitude death window shrinks while if the smaller

sub-population is inactive, the amplitude death window widens as the number of connections is increased.

Rewiring of connection didn't have much effect on the dynamics of the system while the uniform random distribution of external impulses over a range of values widened the amplitude death window.

Therefore, in this thesis, we have observed the collective dynamics of the different systems of coupled model neurons that were intrinsically active or inactive and examined to which state the system converges for different parameter values.

6.2   Future Work

We can extend our system to multi-dimensional networks and study the effect of coupling strength, size of intrinsically active and inactive networks, number of connections, and rewiring of connections between the different networks. Therefore, the collective dynamics of multi-dimensional networks could further be studied.

It would be interesting to perform experiments to see the emergent patterns in multi-dimensional networks.

————————————————————————-

Bibliography

[Avn89] David Avnir, *Chemically induced pulsations of interfaces: The mercury beating heart*, Journal of Chemical Education **66** (1989), no. 3, 211.

[Chi95] Dante R Chialvo, *Generic excitable dynamics on a two-dimensional map*, Chaos, Solitons & Fractals **5** (1995), no. 3-4, 461–479.

[CRBV02] Susana Castillo-Rojas, Guillermina Burillo, and Luis Vicente, *Complex oscillatory behavior of the mercury beating heart system*, The Chemical Educator **7** (2002), no. 3, 159–165.

[Fit61] Richard FitzHugh, *Impulses and physiological states in theoretical models of nerve membrane*, Biophysical journal **1** (1961), no. 6, 445.

[JSGS07] Maruthi Pradeep Kanth Jampa, Abhijeet R Sonawane, Prashant M Gade, and Sudeshna Sinha, *Synchronization in a network of model neurons*, Physical Review E **75** (2007), no. 2, 026215.

[Kan93] Kunihiko Kaneko, *Theory and applications of coupled map lattices*, Nonlinear science: theory and applications (1993).

[KS15] Neeraj Kumar Kamal and Sudeshna Sinha, *Emergent patterns in interacting neuronal subpopulations*, Communications in Nonlinear Science and Numerical Simulation **22** (2015), no. 1-3, 314–320.

[Str01] Stephen Strogatz, *Nonlinear dynamics and chaos: with applications to physics, biology, chemistry, and engineering (studies in nonlinearity)*, Perseus Books Publishing (2001), 505.